

Hydration-Induced Changes of Structure and Vibrational Frequencies of Methylphosphocholine Studied as a Model of Biomembrane Lipids

E. Mrázková,[†] P. Hobza,^{*,†} M. Bohl,[‡] D. R. Gauger,[§] and W. Pohle^{*,§}

The Institute of Organic Chemistry and Biochemistry, Academy of Science of the Czech Republic and Center for Biomolecules and Complex Molecular Systems, Flemingovo nám. 2, 166 10 Praha 6, Czech Republic, Tripos GmbH, Martin-Kollar-Str. 17, D-81829, Munich, Germany, and The Institute of Biochemistry and Biophysics, Friedrich-Schiller University Jena, Hans-Knoell-Str. 2, D-07743 Jena, Germany

Received: March 9, 2005; In Final Form: May 2, 2005

The chemical characteristics of the polar parts of phospholipids as the main components of biological membranes were investigated by using infrared (IR) spectroscopy and theoretical calculations with water as a probe molecule. The logical key molecule used in this study is methylphosphocholine (MePC) as it is not only a representative model for a polar lipid headgroup but itself has biological significance. Isolated MePC forms a compact (folded) structure which is essentially stabilized by two intramolecular C–H···O type hydrogen bonds. At lower hydration, considerable wavenumber shifts were revealed by IR spectroscopy: the frequencies of the (O–P–O)[−] stretches were strongly redshifted, whereas methyl and methylene C–H and O–P–O stretches shifted surprisingly to blue. The origin of both red- and blueshifts was rationalized, on the basis of molecular-dynamics and quantum-chemistry calculations. In more detail, the hydration-induced blueshifts of C–H stretches could be shown to arise from several origins: disruption of the intramolecular C–H···O hydrogen bonds, formation of intermolecular C–H···O_{water} H-bonds. The stepwise disruption of the intramolecular hydrogen bonds appeared to be the main feature that causes partial unfolding of the compact structure. However, the transition from a folded to extended MePC structure was completed only at high hydration. One might hypothesize that the mechanism of hydration-driven conformational changes as described here for MePC could be transferred to other zwitterions with relevant internal C–H···O hydrogen bonds.

Introduction

Living organisms function on the basis of a sophisticated interplay between strictly differentiated constituents (cells, cell organelles), the necessary compartmentization of which is realized by biological membranes. The scaffold of such biomembranes consists of lipid molecules, in many cases with phospholipids as their main components, which are typically assembled as bilayers. Among phospholipids, phosphocholines (PCs) are the most abundant in the plasma membrane of eukaryotes, and, presumably according to a regulatory principle, they occur more in the outer layer. PCs are known to be well hydrated so that their hydration shell prevents other molecules or membranes from approaching. Therefore, the hydration behavior of such lipid systems is of great interest and has been investigated intensely for a number of decades, mainly by experimental means.^{1–4} Water is not only the main ingredient of the natural environment of biomembranes, but it is also particularly well suited to generally probing the interaction potential of lipids.⁵

One of the proven experimental methods in lipid chemistry is infrared spectroscopy,^{6–9} which is, in view of its propensity to characterize hydrogen bonds, especially appropriate for studying water binding to lipids,^{10–13} including the further implications of hydration-triggered solvation phase transitions

on headgroup conformation.^{14,15} However, there are severe limitations to translating IR-spectroscopic data into a basic understanding of the underlying physical background. The possibility to better comprehend such experimental data has been done by an array of theoretical approaches from molecular-mechanics based methods such as molecular dynamics (MD) or Monte Carlo simulations, which are applicable to larger lipid systems,^{16–18} to more sophisticated ab initio quantum chemical calculations performed on model structures of smaller size.^{19–21}

When looking for a key or hinge molecule that would allow a coupled application of IR spectroscopy and ab initio quantum-chemical description in terms of PC hydration, we have logically been attracted to methylphosphocholine (MePC). Its structure, including its atomic numbering, is shown in Figure 1. MePC is not only of academic interest as the PC model per se, but it also occurs naturally in the eggs of sea urchins.²² Moreover, it represents a model of zwitterion molecules that play a fairly important role in many biochemical metabolic processes.

Therefore, we have spectroscopically investigated the hydration of solid deposits of MePC as well as calculated the optimized structures of MePC–water complexes by ab initio quantum chemical methodology. This approach provided a background of solid experimental data and allowed us to follow the related structural and electronic implications of hydration down to the atomistic level. With each method it was possible to adjust the level of singly added water molecules according to increasing hydration number n_w , (the stoichiometric water/lipid ratio) in order to supply directly comparable results. The first preliminary data on MePC hydration, published very recently,²³ have revealed considerable redshifts of the

* Corresponding authors, e-mail: hobza@uochb.cas.cz, wapo@molebio.uni-jena.de

[†] Academy of Science of the Czech Republic and Center for Biomolecules and Complex Molecular Systems.

[‡] Tripos GmbH.

[§] Friedrich-Schiller University Jena.

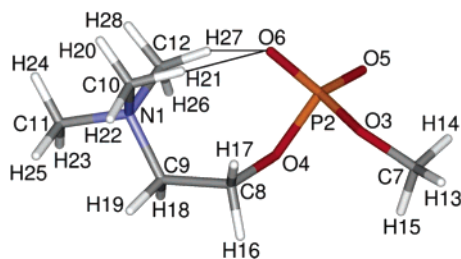


Figure 1. Structure of isolated MePC with numbering of the atoms as used throughout the text; the structure was optimized at the B3LYP/6-31G** level. Intramolecular hydrogen bonds are depicted as lines.

O–P–O[−] stretching vibration bands, ($\nu(\text{O}–\text{P}–\text{O})^-$) and intriguingly large blueshifts of bands arising from the stretching vibrations of methyl and methylene groups ($\nu(\text{C}–\text{H})$).

The observed redshift of the stretching vibrations clearly showed the fingerprint of hydrogen-bond (H-bond) formation. This noncovalent interaction was first described by Linus Pauling in his paper on the nature of chemical bonds in 1931.²⁴ The phenomenon of X–H...Y-type hydrogen bonding, where X is an electronegative element and Y is a place with an excess of electron density, has already been described. The most common types of hydrogen bonds are those containing X, Y = F, O and N, and recently H-bonds of X–H... π (for X = O, C)-type were also reported.^{25,26} The important features of H-bonds are not only the electrostatic interaction but also the transfer of electron density from lone pair orbitals of proton acceptors to the X–H σ^* antibonding orbitals of proton donors, which is a well-known effect in physical organic chemistry called hyperconjugation. A related charge transfer usually does not exceed 0.01 e. The increase in electron density in σ^* antibonding orbitals is accompanied by a weakening of the pertinent bond, which results in elongation of the bond and redshift of the respective stretching vibrations.

On the contrary, to elucidate the observed blueshift represents a more difficult and challenging task because the blueshift can be a consequence of different (i.e., more than two) phenomena. Blueshifted hydrogen bonds of the X–H...Y type have been referred to in the literature many times.^{2–30} It was revealed that their main characteristics are exactly opposite to those of standard hydrogen bonds; the electron density in the X–H σ^* antibonding orbitals decreases upon complex formation, the bond is contracted and the arising stretching vibration is blueshifted. This type of interaction is common in nature, mainly when X is a carbon atom and Y is oxygen,^{31–34} and represents another stabilizing contact apart from standard hydrogen bonding.

In this study we will present more comprehensive experimental data and provide a theoretical explanation for the peculiar spectral behavior observed in the MePC–water systems.

Materials and Methods

Experimental Part. MePC was synthesized ad hoc as previously described.²³ Solid deposits were prepared from aqueous solutions of the material directly on a ZnSe window and investigated spectroscopically in situ in special gas cells. Infrared spectra were recorded by means of an IFS-66 FTIR spectrometer from Bruker (Karlsruhe, Germany) in the DTGS-detection mode using different accumulation rates between 2 and 32 scans at a resolution of 2 cm^{−1}, and a zero-filling factor of 2. Samples were investigated at different values of the surrounding relative humidity (RH) between 0 and 75%, either isopiastically or in nonstationary hydration-dehydration cycles. Increasing the RH to values above 75% resulted, in most cases,

in the MePC film running down the window, thus preventing measurement. This achievable “maximum” hydration level corresponds to an n_w of nearly 6, as could be estimated from the gravimetric curve published by Binder³⁵ very recently. Data processing was done using the OPUS software package (Bruker) with a wavenumber accuracy of 0.1 cm^{−1}. All other experimental details were the same as reported recently.^{12,23}

Molecular Dynamics Simulations. The population of various structures of isolated MePC (cf. Figure 1) in the gas phase was determined by the classical molecular dynamics/quenching (Q) technique, which is a combination of molecular dynamics and minimization. This method was successfully used for sampling of potential energy surface of base pairs³⁶ and details about the technique can be found in ref 36. The MD/Q method was combined with the Cornell et al. force field³⁷ as implemented in AMBER 6.0.³⁸ The missing parameters of MePC were taken from a previously published study³⁹ where they were obtained from ab initio calculations. The TIP3P model of water environment was used in all simulations.

The reliability of the procedure and particularly of the force field was verified by performing the ab initio DFT (density functional theory) MD/Q technique performed using the approximate self-consistent charges tight-binding SCC-DFTB^{40,41} method, which has been shown to provide reliable geometries comparable to high-level ab initio calculations. In contrast to other empirical methods, all parameters are completely calculated within DFT and no fitting is performed, therefore, the major drawback of molecular dynamics with constant charges can be overcome.

The information about hydration sites and conformational changes of MePC was obtained by performing the molecular dynamics simulations with a Cornell et al. force field implemented by our own code into GROMACS.⁴² The charges used in the MD were evaluated for the DFT optimized structure of isolated MePC (cf. Figure 1) using the Merz–Kollman fitting scheme⁴³ (ESP charges) at the HF/6-31G* level. The canonical ensemble was chosen and the temperature of the simulations was set to 300 K. To sample the configuration space properly, the total length of each simulation was 50 ns and the time step used was 0.5 fs.

Quantum Chemistry Calculations. The most populated structures of the MePC–water complexes with $n_w = 1–12$ determined by molecular dynamics simulations were reoptimized at the DFT B3LYP/6-31G** level. For selected structures, the harmonic frequencies were also evaluated. Changes in electron density accompanying complex formation were characterized in terms of natural bond (NBO) analysis.⁴⁴ The NBO analysis also yielded the second-order charge-transfer energy (E2). In all calculations the Gaussian 03 code was used.⁴⁵

For more extended complexes of MePC with water, the quantum mechanical (QM) optimizations were impractical, therefore we used a combined QM/MM approach. The largest complex contained 48 H₂O, the quantum part contained MePC·6H₂O, and the rest of the complex was treated at the molecular mechanics level. Waters in the QM part were selected in order to represent the most abundant motives found in smaller clusters of MePC·H₂O complexes, thus describing properly the first hydration shell. The QM part was described at the B3LYP/6-31G** level (equivalent to previously mentioned clusters), and the molecular mechanics (MM) part was included in Hamiltonian during optimization. To describe the MM part, a Cornell et al. force field with the same parameters as in the MD part was used with the TIP3P water model. The special treatment of the boundary between the QM and MM part was

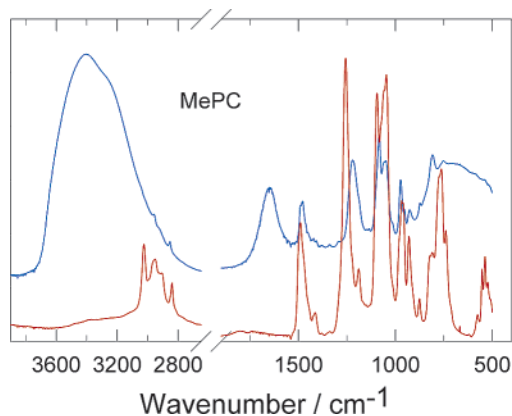


Figure 2. Overall infrared spectra of MePC film measured at 0 (red) and 75% RH (blue).

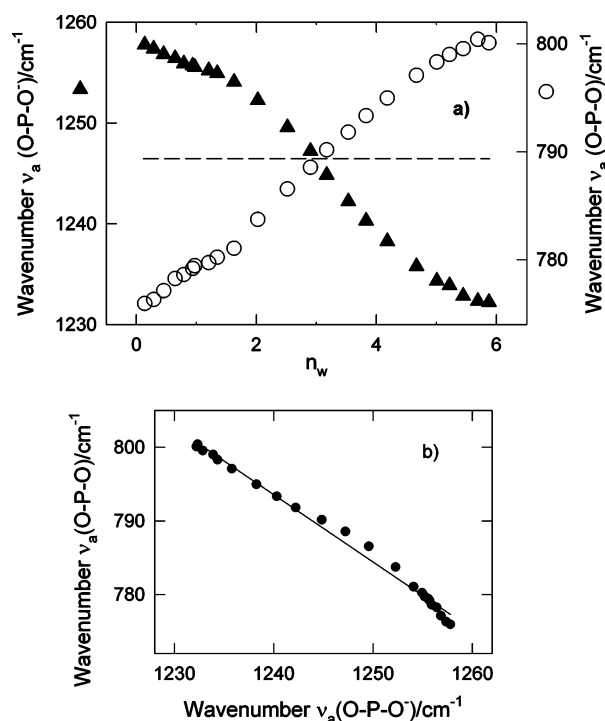


Figure 3. Spectroscopically obtained wavenumber shifts of the antisymmetric stretching vibration bands arising from the phosphate group of MePC, $\nu_a(\text{O-P-O})^-$ and $\nu_a(\text{O-P-O})^-$, as a function of hydration number, n_w ; the horizontal line is a symmetry axis illustrating the correlation existing between both curves (a). Part (b) shows the dependence of these two wavenumber shifts, which are correlated by a very strict linear relationship ($r^2 = 0.992$).

not necessary because the MM part contained only water molecules not chemically bound to the QM system.

Results

FT-IR Spectroscopy. Figure 2 displays the IR spectra of MePC in the dry state (at 0% RH) and in the hydrated state (at 75% RH). Increasing hydration can cause the absorption of the $\nu(\text{O-H})$ band of MePC-associated water near 3400 cm^{-1} , rendering the analysis of $\nu(\text{C-H})$ bands more and more difficult due to band overlap.

In Figure 3, the hydration dependence of the wavenumbers of the phosphate group antisymmetric stretching vibration modes are depicted. The $\nu_a(\text{O-P-O})^-$ band around 1245 cm^{-1} is markedly shifted toward lower frequencies in the same way as was previously observed for the phospholipid phosphate groups^{5,10–13,15,46} as well as in DNA.⁴⁷ Interestingly, this redshift

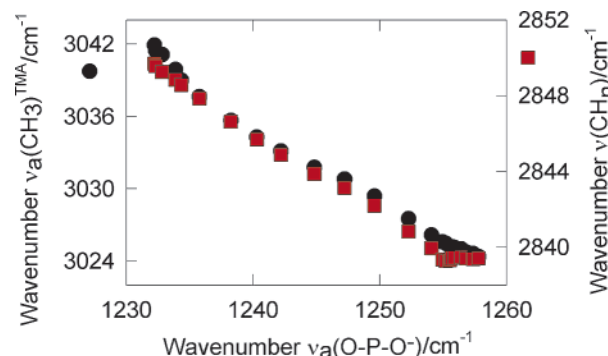


Figure 4. Experimental wavenumbers of two $\nu(\text{C-H})$ bands of MePC (at ~ 2850 and 3040 cm^{-1}) plotted against the iso-humidic wavenumbers of the $\nu_a(\text{O-P-O})^-$ mode.

is accompanied by a hydration-induced blueshift of the anti-symmetric stretching vibration band of the esterified O-P-O bonds ($\nu_a(\text{O-P-O})^-$). This band is located around 790 cm^{-1} in isolated MePC and shifts upon hydration almost about the same magnitude ($\sim 25 \text{ cm}^{-1}$).

Moreover, both curves are evidently correlated with each other because they exhibit the behavior as the reverse images as illustrated by the symmetry axis (dashed line) added in Figure 3a. This is shown even more convincingly by the straight line obtained by plotting the two wavenumbers against one another (cf. Figure 3b).

The symmetric counterparts of both phosphate sub-moieties, $\nu_s(\text{O-P-O})^-$ and $\nu_s(\text{O-P-O})^-$, are shifted into the same directions (to red and blue, respectively), but to a lesser extent (data not shown).

A correlation of the same kind also exists in MePC between the phosphate group on one hand and CH_2 and CH_3 groups on the other, which is documented by the graphs in Figure 4. The largely linear course (consisting of two slight deviations at low and high wavenumbers) of the two curves proves a connection to the influence of bound water molecules onto the MePC phosphate and CH groups. The negative slope of both lines implies that the $\nu_a(\text{O-P-O})^-$ redshift (cf. Figure 3) is again correlated with the synchronous blueshifts of the $\nu(\text{C-H})$ modes, two of which are shown here. These modes refer to bands around 3030 and 2850 cm^{-1} . The 3030 cm^{-1} band is ascribed to the antisymmetric stretching C-H vibration of the methyl groups, whereas the 2850 cm^{-1} band could not be assigned for sure but most probably arises from methylene rather than from methyl groups.

Another finding worth mentioning is the appearance of the maximum and the minimum in the hydration dependencies of the two absorption bands near 1050 and 2950 cm^{-1} at $n_w \sim 1$ (data not shown). This corresponds, in terms of hydration levels, to the slight discontinuities in the courses of the curves included in Figure 3 and in the first figure of ref 5.

Molecular Dynamics Simulations. MD/Q calculations revealed that the global-minimum structure of isolated MePC contains two intramolecular hydrogen bonds that stabilize the geometry and are of key importance for the changes appearing upon hydration. Both moieties ($\text{N}(\text{CH}_3)_3$ and phosphate) were found in close contact so this structure is referred to as a “compact” or “folded” structure throughout the text. The proximity of these moieties is reflected in their through-space N-P distance, and thier value was selected to describe molecular folding (presented in Figure 5). The populations of other structures from MD/Q calculations were considerably lower (by several orders of magnitude), but we are aware that classical MD underestimates the flexibility of the floppy molecules since

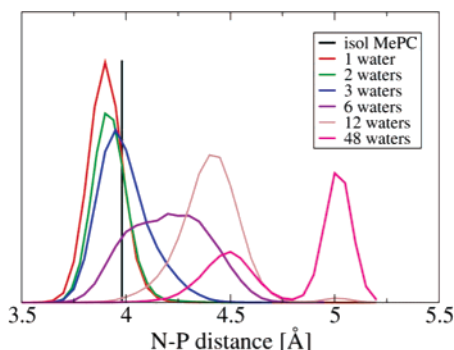


Figure 5. Histogram showing the N–P distances (in Å) for complexes $\text{MePC}\cdots n_w\text{H}_2\text{O}$, $n_w = 1, 2, 3, 6, 12, 48$ (data from MD simulations). The line corresponds to the value of N–P distance in isolated optimized MePC.

constant atomic charges are used. This problem, common for all empirical potentials not using the polarization term, can be overcome by performing *ab initio* MD simulations. The currently used DFTB MD/Q technique showed the existence of more possible conformations; however, the most populated structure again possessed the most important structural motif: two intramolecular hydrogen bonds that play a central role in hydration induced changes.

In the most populated structure of the $\text{MePC}\cdots\text{H}_2\text{O}$ complex found by classical MD, the water molecule formed a hydrogen bond with oxygen O6 of the phosphate group but it did not influence the intramolecular C–H \cdots O distances (C10–H21 \cdots O6 and C12–H27 \cdots O6); they were comparable to distances in isolated MePC. Molecular packing expressed in terms of the N–P distance did not indicate any structural change compared to the isolated MePC (see Figure 5).

The MD revealed that an additional water molecule was bound to an oxygen in the phosphate group. However, even in this case no structural changes appeared to be significant (see Figure 5 with N–P distances).

Further increase of n_w (from 3 to 24) led to a great variety of structures. All structures contained a common motif: water molecules always formed at least two hydrogen bonds with the phosphate group free oxygens (O5 and O6). Apart from the phosphate group, C–H bonds also turned out to bind water by hydrogen bonds. This finding is striking since it reveals, to the best of our knowledge, for the first time that C–H \cdots O hydrogen bonding was observed in lipids or structures that could mimic lipids. Previously, this type of binding was reported to exist in organic molecules as well as other biomolecules (proteins, nucleic acids, carbohydrates).⁴⁸ Moreover, the water molecules interacted among themselves by H-bonds as well, thus creating a network around MePC.

Another ubiquitous feature common to all structures of the MePC–water complexes with n_w of 1–24 was the increase of the C–H \cdots O intramolecular distances. It obviously signals the partial unfolding of the original structure (compare the N–P distances presented in Figure 5). The MD simulations in this case showed that one intramolecular hydrogen bond was completely disrupted (it could be either C10–H21 \cdots O6 or C12–H27 \cdots O6 without any preference), whereas the second one remained as a weaker contact.

The largest complex investigated contained 48 water molecules and thus the first, second, and part of the third solvation shells were present. It was found that no intramolecular hydrogen bonds were present and the structure of MePC proved to be fully unfolded. In such a structure all three methyl groups of the $-\text{N}(\text{CH}_3)_3$ moiety behaved the same way.

To summarize, the molecular-dynamics simulations clearly indicated how the conformation of MePC is sensitive to hydration. It was shown that upon progressive hydration the conformation of MePC is modified from a closely folded to a fully extended one. Note that similar conformational changes could be induced without introducing a water environment simply by increasing the temperature (data not shown); the MD simulations proved this phenomenon when the temperature was set to 400 K.

Quantum Chemical Calculations. Isolated MePC. The structure of isolated gas-phase MePC is presented in Figure 1 and the respective bond lengths together with selected angles and N–P distance are collected in Supporting Information.

The H \cdots O(P) distances between atoms involved in intramolecular hydrogen bonds were 1.990 Å (C10–H21 \cdots O6) and 2.038 Å (C12–H27 \cdots O6). Related to what is usually found in C–H \cdots O hydrogen bonds (mostly between 2.2 and 2.5 Å),⁴⁵ these H \cdots O distances are strikingly short, which is in favor of a high stability of the intramolecular H-bonds in MePC. Both intramolecular contacts possessed all the crucial characteristics of hydrogen bonding, the most prominent being the hyperconjugation among lone pairs of phosphate oxygen and σ^* antibonding orbitals of the C–H-bonds. One of the most useful quantities for providing information about the strength of the hydrogen bonding was the E2 energy which was, in the case of LP O6 $\rightarrow \sigma^*$ C10–H21 hyperconjugation, equal to 11.54 kcal.mol^{−1}, and 9.00 kcal.mol^{−1} for LP O6 $\rightarrow \sigma^*$ C12–H27. According to the known effects of hyperconjugation, the increase of electron density in the antibonding orbital (in these cases the values range between 0.02 and 0.03 e) must be accompanied by elongation of the respective bond; and indeed C10–H21 and C12–H27 bonds were found to be the longest C–H bonds in the respective methyl groups. Both hydrogen bonds mentioned were responsible for the particular stability of the structure; the barrier for free rotation of $-\text{N}(\text{CH}_3)_3$ moiety reached approximately 8 kcal.mol^{−1}.

The optimized structure of isolated MePC obtained in this work and shown in Figure 1 is in good agreement with other DFT and Hartree–Fock computations.²¹ The two intramolecular hydrogens bond with one of the phosphate oxygens and the reported hydrogen bond distances are very consistent with our findings.

MePC $\cdots\text{H}_2\text{O}$. The structure of optimized $\text{MePC}\cdots\text{H}_2\text{O}$ complex is depicted in Figure 6a. The bond lengths and angles are again collected in Supporting Information.

It is well known that the phosphate group of MePC was the preferred binding site for water molecules. The P–O6 bond involved in hydrogen bonding of the first water molecule was elongated, whereas the P–O5 bond, without any intermolecular contact, was found to be shortened (see Supporting Information). The explanation for this phenomenon can be proven by virtue of electron-density changes connected with complex formation. In the first step, the electron density was transferred from the lone electron pair of O6 by the formation of a hydrogen bond with a water molecule. Consequently, the loss was compensated for by the σ^* P–O5 antibonding orbital because exceptionally strong electron delocalization among all phosphate group orbitals occurred. Thus the decrease in electron density of the σ^* P–O5 antibonding orbital was followed by observed strengthening and contraction of the bond.

However, the electron density changes in the phosphate moiety were discovered to be rather complex and cohesive and were also reflected in the O3–P2–O4 (ester) and O5–P2–O6 bond angles. The O3–P2–O4 (ester) angle increased upon

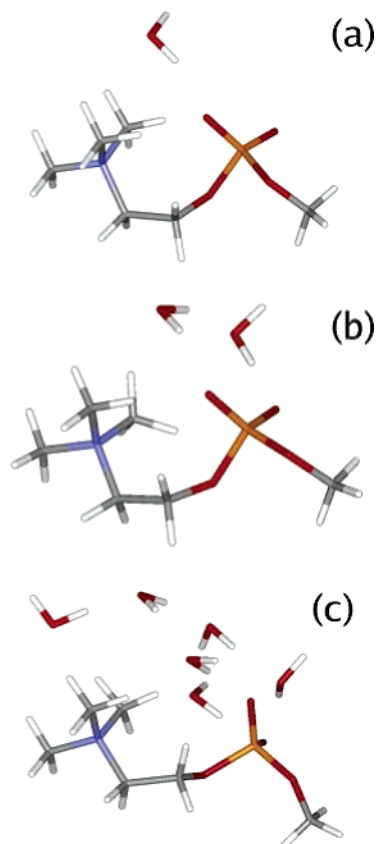


Figure 6. Optimized structures of MePC complexes with 1, 2 and 6 H₂O (a–c).

hydration, whereas the O5–P2–O6 angle decreased (cf. Supporting Information). The variation in bond lengths affected the vibrational frequency of the antisymmetric $\nu(\text{O}=\text{P}=\text{O})$ stretch, which was blueshifted in agreement with experimental spectra (cf. Figure 3a). The theoretical explanation of such behavior is currently impractical due to complicated coupling among all orbitals of the phosphate group.

The hydrogen-bond formation with one water molecule did not affect the distances of the intramolecular hydrogen bonds. However, both intramolecular contacts were weakened substantially upon complex formation; the respective E2 charge-transfer energies decreased by about 25% in the case of C10–H21...O and by about 60% in the case of C12–H27...O. Accordingly, the electron density in both the σ^* antibonding orbital of C10–H21 and C12–H27 bonds was reduced by about 0.005 e in the former case and by about 0.01 e in the latter case. The decrease in electron density caused the contraction of both bonds (see Supporting Information) and a blueshift of the respective stretching vibrations (see Table 1). Because a larger decrease in electron density occurred in the C12–H27 bond, its $\nu(\text{C}=\text{H})$ band was significantly more shifted than that of the C10 methyl group.

In addition, we found that, apart from the C10–H21 and C12–H27 bonds, the C10–H20 and C12–H28 bonds were also affected by hydration (see Supporting Information). The latter C–H bonds interacted directly with water oxygen and their bond lengths were found to be contracted.

Surprisingly, the effect of binding one water molecule was also observed in the C7 methyl group and the C8 methylene group. The bonds were contracted (see again Supporting Information) without being in direct contact with either water or phosphate oxygens. This was explained by the remarkably intense hyperconjugative interaction among the antibonding

TABLE 1: Calculated Wavenumbers (ν , in cm^{-1}) of Vibrational Stretching Modes for Selected Groups of MePC and Their Hydration-Induced Shifts

	MePC	$\Delta\nu$		
		MePC...H ₂ O	MePC...2H ₂ O	MePC...6H ₂ O
C12 methyl	3 187	48	43	58
C10 methyl	3 165	22	27	–4
C12 methyl	3 150	45	30	53
C7 methyl	3 132	5	8	17
C10 methyl	3 132	24	15	23
C7 methyl	3 097	6	14	20
C8 methylene	3 089	6	13	11
C12 methyl	3 047	48	31	60
C7 methyl	3 021	5	14	9
C10 methyl	3 007	46	38	44
C8 methylene	2 997	8	22	33
$\nu_a(\text{O}=\text{P}=\text{O})^-$	1 314	–4	–41	–53
$\nu_a(\text{O}=\text{P}=\text{O})$	752	11	25	26

orbitals of the C–H bonds and the phosphate oxygen lone pairs, the P2–O6 antibonding orbital and the lone pairs of O3 and O4.

MePC...2H₂O. Increasing the hydration number to 2 resulted in further geometrical changes. The most populated structure from the MD simulation characterized by the presence of two hydrogen bonds between two waters and the two phosphate free oxygens was reoptimized, and its geometry is depicted in Figure 6b.

The optimized geometry is largely in agreement with the crystal structure of DMPC reported by Hauser et al.⁴⁹ (DMPC crystallizes with 2H₂O, therefore data for crystal DMPC are not available.) In contrast to the MePC...H₂O complex, the P–O6 bond length changed only slightly (contraction by about 0.007 Å), whereas the P–O5 bond lengthened significantly (by about 0.017 Å), which was also reflected in both the antisymmetric bands (compare 41 to 4 cm^{-1} in the case of MePC...H₂O).

Formation of phosphate...water hydrogen bonds clearly had an impact on the strength of both intramolecular contacts. The E2 (LP O6 \rightarrow σ^* C12–H27) energy decreased dramatically when compared to an isolated system, which showed that the intramolecular bond was practically disrupted. The consequences were straightforward: the electron density in the σ^* C12–H27 antibonding orbital decreased by about 0.02 e, this bond was contracted by about 0.008 Å, and the respective stretching vibration was blueshifted (cf. Table 1). The second intramolecular hydrogen bond remained; however, it became weaker (E2 energy decreased by about 20%). The shifts of related stretching-vibration frequencies are presented in Table 1.

Hyperconjugation among phosphate-oxygen lone-pair orbitals, the P2–O6 σ^* antibonding orbital, and the σ^* antibonding orbitals of C8–H16,17 and C7–H13,14,15 bonds in the MePC...2H₂O complex was more intense than in the MePC...H₂O complex, but the general characteristics remained similar. Stronger changes in electron density were followed by larger blueshifts of the stretching vibrations (see Table 1), and such a predicted increase was fully confirmed experimentally.

In the MePC...2H₂O complex, interactions between water molecules and C–H bonds (namely C10–H20 and C12–H28) were again detected. Both of these C–H bonds mentioned were slightly contracted compared to isolated MePC (by about 0.003 Å for C10–H20 and 0.001 Å for C12–H28, see also Supporting Information).

Figure 7 shows a superimposition of the DFT-optimized structures of MePC and its monohydrates and dihydrates. The

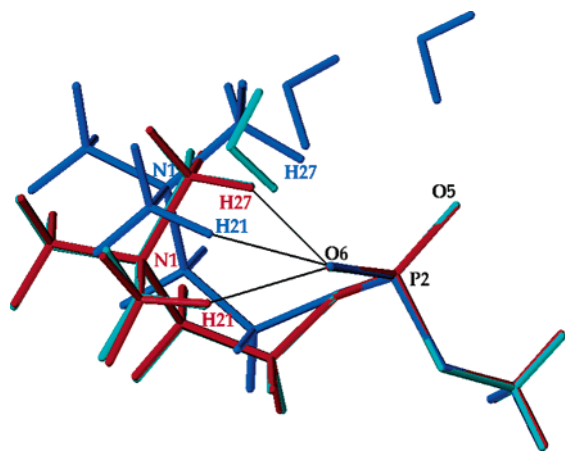


Figure 7. Superposition of DFT-optimized systems of MePC with zero, one, and two water molecules coded by the colors red, cyan, and blue, respectively; the five phosphate atoms were used to align the structures. The intramolecular hydrogen bonds are indicated by thin black lines.

picture illustrates the features of the intramolecular H-bonding of isolated MePC, the positions of the water molecules, and, in particular, the conformational differences with respect to the $-\text{N}(\text{CH}_3)_3$ orientation. In the case of two water molecules bound to phosphate, the $\text{C12}-\text{H27}\cdots\text{O6}$ hydrogen bond was disrupted. Such an effect could be attributed to a hydration-induced increase of the conformational flexibility of the $-\text{N}(\text{CH}_3)_3$ moiety.

MePC $\cdots n_w\text{H}_2\text{O}$ ($n_w = 3-12$). MD simulations performed on these complexes pointed out a great variety of interchangeable hydration sites, so it was necessary to investigate more structures (4 or 6 structures per n_w). An example of the investigated structures (MePC $\cdots 6\text{H}_2\text{O}$ complex) is depicted in Figure 6c.

One of the most common features for all complexes was the presence of at least two hydrogen bonds between phosphate and water molecules. Some structures contained more than one hydrogen bond between one of the phosphate oxygens and the water molecules, but the P–O bond was not further lengthened. This was evident when considering the decrease in the P–O electron density, which was, in all cases, approximately 0.015 e (independent of the number of hydrogen bonds). Accordingly, the P2–O5 and P2–O6 bonds of the phosphate group possessed similar bond lengths in all these structures and exhibited similar calculated redshifts (see Supporting Information). This finding fully agrees with experimental results in terms of the $\nu_a(\text{O}-\text{P}-\text{O})^-$ mode (see Figure 3a).

Because the formation of more than two hydrogen bonds did not cause further decrease in electron densities of phosphate free-oxygen lone pairs, the electron-density “flow” from antibonding orbital P2–O6, lone pairs of O3 and O4, and C8–H16,17 and C7–H13,14,15 σ^* antibonding orbitals remained at the same level as in the case of MePC $\cdots 2\text{H}_2\text{O}$. Consequently, a further strong increase in the stretching vibrations of the C8 methylene and C7 methyl groups was not detected.

As mentioned previously, not only did the phosphate group provide hydration sites, but large numbers of structures also contained an unexpected direct $\text{C}-\text{H}\cdots\text{O}_{\text{water}}$ motif. The typical range of the $\text{C}-\text{H}\cdots\text{O}$ distances was from 2.1 to 2.7 Å. The blueshifts of the C–H vibrational frequencies of these methyl groups were strongly dependent on the positions of waters and varied from ~ 25 to $\sim 70\text{ cm}^{-1}$. The largest shift occurred when a water molecule formed an almost linear $\text{C}-\text{H}\cdots\text{O}$ contact, which possessed all the characteristics of a blueshifting hydrogen bond. Hyperconjugation appeared between C–H σ^* antibonding orbitals and lone pairs of water oxygen, thus the electron density

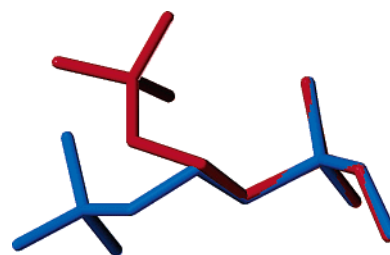


Figure 8. Superposition of the structures of MePC without water (DFT-optimized) and under the influence of 48 water molecules (not shown) obtained by the QM/MM approach coded by the colors red and blue, respectively; the five phosphate atoms were used to align the structures.

in C–H σ^* antibonding orbitals decreased. This bond was shortened and the resulting stretching vibration was blueshifted. If such a contact was not formed, only a moderate blueshift appeared as a consequence of electrostatic interaction.

The intramolecular hydrogen bonds were influenced by the first solvation shell (3–12 waters) in the same way as by two bound water molecules: one intramolecular hydrogen bond was disrupted (can be either $\text{C10}-\text{H21}\cdots\text{O6}$ or $\text{C12}-\text{H27}\cdots\text{O6}$), while the second one remained; however, it was somewhat weaker. The observed blueshifts of C–H bonds reflected the presence or absence of an intramolecular hydrogen bond.

MePC $\cdots 48\text{H}_2\text{O}$. Forty-eight water molecules formed the first, second, and part of the third solvation shell. The picture in Figure 8 where hydrogen atoms and water molecules were omitted for the sake of clarity demonstrates that under such conditions MePC is fully extended and no intramolecular C–H \cdots O hydrogen bonds were detected. The folded structure of MePC in the absence of water (DFT-optimized) with an N–P distance of 3.98 Å is compared with the unfolded structure found in the presence of 48 water molecules (QM/MM-optimized) with an N–P distance of 4.67 Å. The substantial conformational change of the whole MePC backbone structure connected with unfolding and N–P separation is clearly illustrated in Figure 8. The optimization showed further contraction of all C–H bonds compared to lower hydration (in the presence of only the first solvation shell); the contraction varied from -0.003 to -0.011 Å depending on the position of the water molecule in the quantum part.

The changes in electron density could be examined based on ESP charges (see Table 2). If the structure was completely unfolded and water molecules were not explicitly taken into account (third column in Table 2), all hydrogen atom charges of the methyl groups became roughly equivalent and any observed charge changes of the phosphate moiety were not substantial. However, explicitly considered water molecules influenced the ESP charges of MePC extensively (second column in Table 2), which clearly indicated that the main electron density changes were induced by the interaction with the water shell and not only by a conformational change.

Discussion

Blueshifts of the C–H Stretching Vibration Bands. Isolated MePC has turned out to adopt a compact structure. Such a structure was recently proposed for related systems, e.g., diacyl-PC, and electrostatic attraction between negatively charged phosphate and positively charged $-\text{N}(\text{CH}_3)_3$ mainly accounted for its stabilization.²⁰ Our computations have clearly revealed that isolated MePC is essentially stabilized by two relatively strong intramolecular C–H \cdots O hydrogen bonds. Accordingly, both C10–H21 and C12–H27 bonds possess an exceptional characteristic: they were the longest of all C–H

TABLE 2: ESP Charges of MePC in Isolated State, in Complex with 48 H₂O (structure taken from QM/MM) Where Water Molecules Were Explicitly Taken into Account and Charges Corresponding to Unpacked Structure of MePC in Complex MePC...48H₂O without Taking Water Molecules into Account (in table named “unpacked structure”)

	MePC	MePC...48H ₂ O ^a	unpacked structure
N1	0.286	-0.836	0.245
P2	1.369	1.123	1.289
O3	-0.461	-0.496	-0.503
O4	-0.614	0.568	-0.589
O5	-0.756	-0.647	-0.794
O6	-0.861	-0.935	0.813
C7	-0.059	0.016	0.142
C8	0.418	-1.453	0.359
C9	-0.359	0.924	-0.191
C10	-0.473	-2.727	-0.485
C11	-0.511	0.030	-0.371
C12	-0.309	-0.874	-0.474
H13	0.083	0.063	0.056
H14	0.104	0.067	0.006
H15	0.063	0.100	0.034
H16	0.028	0.315	0.031
H17	-0.032	0.403	-0.007
H18	0.185	0.150	0.158
H19	0.133	0.109	0.087
H20	0.172	1.058	0.193
H21	0.316	0.988	0.206
H22	0.174	0.757	0.202
H23	0.191	-0.022	0.227
H24	0.206	0.325	0.157
H25	0.201	0.136	0.184
H26	0.158	0.176	0.266
H27	0.213	0.844	0.203
H28	0.133	0.203	0.181

^a This case gives evidence about changes in charges (or in electron density) induced only by conformational transition.

bonds within the -N(CH₃)₃ moiety. Due to the hyperconjugation interaction described above, the electron density in C10-H21 and C12-H27 σ^* antibonding orbitals exhibited higher values compared to other C-H bonds. In the absence of H-bonds, such as O-H...O or O-H...N, which do not exist in MePC or in diacyl-PCs, C-H...O hydrogen bonds can become a determining structural factor in biomolecules,^{46,47} despite their weaker strength. This might be structurally meaningful only for MePC and for diacyl-PCs comprised in biomembranes. Moreover, one could speculate whether the structural unfolding induced by water or, more specifically, by some effector, could be regarded as a general regulatory element for biologically relevant zwitterions having intramolecular C-H...O hydrogen bonds.

Upon hydration, both methyl groups involved in intramolecular hydrogen bonds exhibited an interesting behavior. Although the distance between the C10-H21 and C12-H27 hydrogens and oxygen O6 remained almost the same in the first stage of the hydration process (1 and 2 waters), the bonds became weaker compared to isolated MePC. Accordingly, the electron density in the C-H σ^* antibonding orbitals decreased and a concomitant blueshift of stretching vibrations was evident in both IR spectroscopy and theoretical vibrational analysis. It was found that the first and second water molecules had already initiated the hydration-induced changes of MePC to a large extent. However, our calculations showed that complete disruption of both intramolecular hydrogen bonds is completed only at high hydration (also including the second and a part of the third hydration shells) and the resulting relative strengthening of these C-H bonds was subsequently demonstrated by the further blueshift of the C-H stretching vibrations.

This work is in line with the conclusions drawn from previous NMR spectroscopic studies on the hydration of diacyl PCs with isotope-labeled headgroups which revealed, at large n_w , a movement of the -N(CH₃)₃ end of choline away from the hydrocarbon layers more toward the aqueous phase,⁴⁹ i.e., an expansion of the PC structure.⁵⁰

Unexpectedly, hyperconjugation existed not only among the phosphate group orbitals but also among phosphate and C8-H16,17 and C7-H13,14,15 σ^* antibonding orbitals. This resulted in an electron-density “flow” from C8-H16,17 and C7-H13,14,15 orbitals, which compensated for the loss of electron density in the phosphate moiety. The electron-density “flow” described represents the only explanation for the contraction and blueshifts of C8-H16,17 and C7-H13,14,15 stretching frequencies. Because of the close connection between C8 methylene and C7 methyl groups and the phosphate moiety, the dependence of frequency shifts upon hydration also correlates. The most significant shift was observed in complexes containing 2–3 water molecules; shifts upon higher hydration (involving the second solvation shell) were only moderate.

Hydration-Induced Changes in the Phosphate Moiety. The phosphate moiety is a strong proton acceptor forming hydrogen bonds with water molecules upon hydration. The main characteristic of this process is the loss of electron density of the P-O bond(s) due to very strong hyperconjugation with the O-H σ^* antibonding orbital of water and consequently the elongation and redshift of (O-P-O)⁻ stretching vibrations. This redshift is only moderate under very low hydration (one water molecule) because of electron density compensation and becomes larger when the electron density loss appearing due to the formation of another hydrogen bond could not be compensated for within the same scope. The formation of more than one hydrogen bond per phosphate oxygen was not followed by further dramatic loss in electron density; thus, further redshift is increasingly less pronounced.

Simultaneously, and less easily predicted, the O-P-O stretching vibrations underwent, upon hydration, remarkable blueshifts. A straightforward theoretical explanation for the blueshifts of the $\nu(\text{O-P-O})$ modes is, unfortunately, not possible at the present stage. This is due to the complicated coupling existing among all orbitals of the phosphate group.

The IR spectroscopic measurements of MePC deposits under very high hydration could not be performed for the reasons described above in the Materials and Methods section. Studies with aqueous dispersions of 1,2-diacyl PCs^{13,51} showed antisymmetric (O-P-O)⁻ stretches around 1225 cm⁻¹. They tended to have values below the 1230 cm⁻¹ band obtained for MePC at the highest $n_w = 6$ achievable under our experimental conditions (see Figure 2) as well as for hydrated multilayers of diacyl PCs.^{12,43,52} Thus, a hydration up to levels as high as those generated by the MD simulations may result in a further lowering of the wavenumber of the antisymmetric O-P-O⁻ stretch.

Last, we would like to refer to the bond angles $\alpha(\text{O-P-O})^-$ and $\alpha(\text{O-P-O})$, which also indicate structural changes.⁵³ Their behavior in terms of hydration (see Figure 9) is perfectly in parallel to that of the wavenumbers (Figure 3). So, in both instances the first water did not affect any of these angles very much, while it was the second and also the third added water molecule that exerted a strong influence. These findings are very much in accordance also with the structures given in Figure 7, revealing that a significant conformational change of the MePC backbone occurs only in the MePC...2H₂O complex.

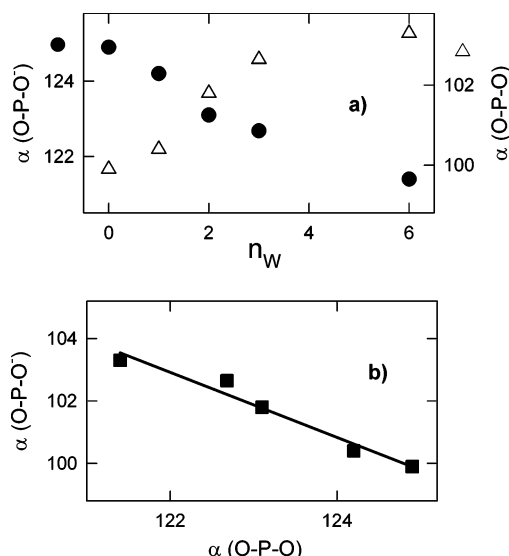


Figure 9. Hydration dependencies of the O-P-O⁻ and O-P-O phosphate angles ($\alpha(\text{O-P-O}^-)$ and $\alpha(\text{O-P-O})$), as derived from the DFT-optimized structures (a). Part (b) shows the dependence of these two angles which are correlated by a linear relationship ($r^2 = 0.964$).

The hydration-induced decrease of $\alpha(\text{O-P-O}^-)$ was expected due to the decrease of the electron density of these P-O bonds caused by hydrogen-bonded water molecules. It was also accompanied by a synchronous increase of $\alpha(\text{O-P-O})$. Owing to their reversed-image shapes (Figure 9a), it is evident that both functions are again correlated. This is corroborated by the nearly ideally linear course of the plot correlating the two angles with each other (see Figure 9b).

Correlation of Hydration-Driven Structural Changes in MePC. Our IR-spectroscopic data have revealed that the structural implications owing to the (low) hydration of MePC are essentially characterized by strict correlations between the n_w dependencies of the wavenumbers of several modes. This appears to hold true for correlations involving both phosphate (O-P-O⁻ and O-P-O); and phosphate and methyl/methylene groups (shown in Figures 3 and 4, respectively). In the former case, such a relationship was also indicated by theoretical results (Figure 9). The course of the respective curves is sigmoidal and can be consistently described by a sequence of ranges with small (until $n_w = \sim 1$), strong (n_w of 2–3), and again small slopes ($n_w = \sim 4$ and higher). The sigmoidal shape of these dependencies is typical just for MePC; it was generally not observed for the diacyl PCs studied before.^{12,43,52}

The same picture of correlation between dependencies of the wavenumbers of several modes upon hydration was obtained by theoretical calculations. Even though the ab initio calculations did not provide quantitative agreement with IR study, the trends observed are consistent with experiment and therefore are in favor of the theoretical explanation of the observed wavenumber shifts based on electron density changes.

We are aware that very low hydration conditions are not relevant to a biological model of a membrane for which only a high hydration state is relevant. These calculations were performed in order to reproduce the IR experiments carried out at 0% RH.

Temperature Dependence. It should be noted that similar structural changes (from a compact structure to a fully unfolded one) as evoked by hydration could also be induced by raising the temperature (MD simulations, not presented). The heat supplied to the system leads to extension of the packed structure as well.

Conclusions

The results obtained by a combined use of IR spectroscopy and theoretical calculations clearly show the fundamental role of hydration on the structural characteristics of MePC. The progress of hydration can be described as follows:

(1) The Effect of Very Low Hydration (1 or 2 waters). At very low hydration, MePC molecules exist in a compact structure; however, the intramolecular hydrogen bonds are weaker than in the isolated state. The free oxygens of the phosphate group form H-bonds with water molecules and, consequently, the $\nu(\text{O-P-O}^-)$ modes exhibit redshifts. On the contrary, the C10 methyl and the C12 methyl groups exhibit blueshifts of their vibrational stretching frequencies due to the weakening of intramolecular hydrogen bonds with the phosphate group. The interaction with water is also connected with electron-density transfer, which is intermolecular as well as intramolecular. Electron-density transfer among orbitals was found to be responsible for geometrical changes not only in the phosphate moiety or in C-H bonds interacting with the phosphate group or with bound water but also for other parts of MePC that are not involved in direct interaction with water. These transitions probably do not occur in a biomembrane that is always hydrated. The simulations were performed in order to reproduce IR experiments carried out at 0% RH.

(2) The Effect of Low and Intermediate Hydration (First Solvation Shell Is Present). The structure of MePC interacting with 3–12 water molecules becomes increasingly more extended than in an isolated or very low hydrated state. The partial extension appears to be due to the further weakening of the first intramolecular hydrogen bond and to the disruption of the second one.

(3) The Effect of Strong Hydration (the Second and Part of the Third Solvation Shells Are Present). In a fully hydrated MePC system, the transition from a compact to an unfolded conformation is completed. Intramolecular hydrogen bonds do not exist and all methyl groups become equivalent, which leads to increased conformational freedom. The electron-density properties of extended MePC are influenced mainly by its interaction with water molecules in a global sense and not only by conformational changes.

Acknowledgment. This work was part of the research project Z40550506 and was supported by the Grant Agency of the Czech Republic (grant No. 203/05/0009, E.M. and P.H.) and MSMT CR (grant No. LC 512).

Supporting Information Available: Table S1: bond lengths, values of N-P distances (in Å) and of selected bond angles (in deg) of MePC, and their changes for complexes $\text{MePC} \cdots n_w \text{H}_2\text{O}$; $n_w = 1, 2, 6, 12$, and 48. Table S2: Calculated wavenumbers (ν in cm^{-1}) of vibrational stretching modes for selected groups of MePC and their hydration-induced shifts. This material is available free of charge via the Internet at <http://pubs.acs.org>.

References and Notes

- (1) Hauser, H. "Lipids" in *Water – A Comprehensive Treatise*; Franks, F.; Plenum Press: New York, 1975; p 209.
- (2) Rand, R. P.; Parsegian, V. A. *Biochim. Biophys. Acta* **1989**, 988, 351.
- (3) McIntosh, T. J.; Magid, A. D. "Phospholipid hydration" in *Phospholipids Handbook*; Cevc, G.; Marcel Dekker: New York, 1993; p 553.
- (4) Milhaud, J. *Biochim. Biophys. Acta* **2004**, 1663, 19.
- (5) Pohle, W.; Gauger, D. R.; Bohl, M.; E. Mrázková, E.; Hobza, P. *Biopolymers* **2004**, 74, 27.

- (6) Fringeli, U. P.; Günthard, H. H. in *Membrane Spectroscopy*; Grell, E., Ed.; Springer-Verlag: Berlin, 1981; p 270.
- (7) Lee, D. C.; Chapman, D. *Biosci. Rep.* **1986**, *6*, 235.
- (8) Mantsch, H. H.; McElhaney, R. N. *Chem. Phys. Lipids* **1991**, *57*, 213.
- (9) Chalmers, J. M.; Griffiths, P. R., Eds.; *Handbook of Vibrational Spectroscopy*, John Wiley & Sons: Chichester, 2002, p 3447.
- (10) Bertoluzza, A.; Bonora, S.; Fini, G.; Morelli, M. A. *Can. J. Spectrosc.* **1984**, *29*, 93.
- (11) Wong, P. T. T.; Mantsch, H. H. *Chem. Phys. Lipids* **1988**, *46*, 213.
- (12) Pohle, W.; Selle, C.; Fritzsche, H.; Binder, H. *Biospectrosc.* **1998**, *4*, 267.
- (13) Hübner, W.; Blume, A. *Chem. Phys. Lipids* **1998**, *96*, 99.
- (14) Pohle, W.; Selle, C. *Chem. Phys. Lipids* **1996**, *82*, 191.
- (15) Binder, H.; Pohle, W. *J. Phys. Chem. B* **2000**, *104*, 12039.
- (16) Pastor, R. W. *Curr. Opin. Struct. Biol.* **1994**, *4*, 486.
- (17) Tieleman, D. P.; Berendsen, H. J. C. *J. Chem. Phys.* **1996**, *105*, 4871.
- (18) De Vries, A. H.; Mark, A. E.; Marrink, S. J. *J. Am. Chem. Soc.* **2004**, *126*, 4488.
- (19) Peinel, G.; Frischleder, H. *Chem. Phys. Lipids* **1979**, *24*, 277.
- (20) Hadzi, D.; Hodoscek, M.; Grdadolnik, J.; Aybelj, F. *J. Mol. Struct.* **1992**, *266*, 9.
- (21) Hill, J. R.; Liang, C. *Ber. Bunsenges. Phys. Chem.* **1997**, *101*, 1828.
- (22) Szwergold, B. S.; Kappler, F.; Cohen, L. H.; Nanavati, D.; Brown, T. R. *Biochem. Biophys. Res. Commun.* **1990**, *172*, 855.
- (23) Pohle, W.; Gauger, D. R.; Fritzsche, H.; Rattay, B.; Selle, C.; Binder, H.; Boehlig, H. *J. Mol. Struct.* **2001**, *463*, 563.
- (24) Pauling, L. *J. Am. Chem. Soc.* **1931**, *53*, 1367.
- (25) Jeffrey, G. A. *An Introduction to Hydrogen Bonding*; Oxford University Press: New York, 1997.
- (26) Scheiner, S. *Hydrogen Bonding*; Oxford University Press: New York, 1997.
- (27) Budešinsky, M.; Fiedler, P.; Arnold, Z. *Synthesis Stuttgart* **1989**, *11*, 858.
- (28) Boldeskul, I. E.; Tsymbal, I. F.; Ryltsev, E. V.; Latajka, Z.; Barnes, A. J. *J. Mol. Struct.* **1997**, *436*, 167.
- (29) Hobza, P.; Špirko, V.; Selzle, H. L.; Schlag, E. W. *J. Phys. Chem. A* **1998**, *102*, 2501.
- (30) Hobza, P.; Havlas, Z. *Chem. Rev.* **2000**, *100*, 4253.
- (31) Hiroatsu, M.; Yoshida, H.; Hieda, H.; Yamanaka, S.-y.; Harada, T.; Shin-ya, K.; Ohno, K. *J. Am. Chem. Soc.* **2003**, *125*, 13910.
- (32) Cordier, F.; Barfield, H.; Grzesiek, S. *J. Am. Chem. Soc.* **2003**, *125*, 15750.
- (33) Panza, L.; Martini, G.; Rossi, C. *J. Am. Chem. Soc.* **2002**, *124*, 8778.
- (34) Arbely, E.; Arkin, I. T. *J. Am. Chem. Soc.* **2004**, *126*, 5362.
- (35) Binder, H. *Appl. Spectrosc. Rev.* **2003**, *38*, 15.
- (36) Kabeláč, M.; Hobza, P. *J. Phys. Chem. B* **2001**, *105*, 5804.
- (37) Cornell, W. D.; Cieplak, P.; Bayly, C. I.; Gould, I. R.; Merz, K. M.; Fergusson, D. M.; Spellmeyer, D. C.; Fox, T.; Caldwell, J. W.; Kollman, P. A. *J. Am. Chem. Soc.* **1995**, *117*, 5179.
- (38) Case, D. A.; Pearlman, D. A.; Caldwell, J. W.; Cheatham, T. E., III; Wang, J.; Ross, W. S.; Simmerling, C. L.; Darden, T. A.; Merz, K. M.; Stanton, R. W.; Cheng, A. L.; Vincent, J. J.; Crowley, M.; Tsui, V.; Gohlke, H.; Radmer, R. J.; Duan, Y.; Pitera, J.; Massova, I.; Seibel, G. L.; Singh, U. C.; Weiner, P. K.; Kollman, P. A. *AMBER 6.0*; University of California: San Francisco, 2002.
- (39) Řeha, D.; Kabeláč, M.; Ryjáček, F.; Šponer, J.; Šponer, J. E.; Elstner, M.; Suhai, S.; Hobza, P. *J. Am. Chem. Soc.* **2002**, *124*, 3366.
- (40) Elstner, M.; Hobza, P.; Frauenheim, T.; Suhai, S.; Kaxiras, E. *J. Chem. Phys.* **2001**, *114*, 5149.
- (41) Elstner, M.; Porezag, D.; Jungnickel, G.; Elsner, J.; Haugk, M.; Frauenheim, T.; Suhai, S.; Seifert, G. *Phys. Rev. B* **1998**, *58*, 7260.
- (42) Lindahl, E.; Hess, B.; van der Spoel, D. *GROMACS 3.0 J. Mol. Model.* **2001**, *7*, 306.
- (43) Besler, B. H.; Merz, K. M., Jr.; Kollman, P. A. *J. Comput. Chem.* **1990**, *11*, 431.
- (44) Foster, J. P.; Weinhold, F. *J. Am. Chem. Soc.* **1980**, *102*, 7211.
- (45) Frisch, M. J.; Trucks, G. W.; Schlegel, H. B.; Scuseria, G. E.; Robb, M. A.; Cheeseman, J. R.; Montgomery, Jr., J. A.; Vreven, T.; Kudin, K. N.; Burant, J. C.; Millam, J. M.; Iyengar, S. S.; Tomasi, J.; Barone, V.; Mennucci, B.; Cossi, M.; Scalmani, G.; Rega, N.; Petersson, G. A.; Nakatsuji, H.; Hada, M.; Ehara, M.; Toyota, K.; Fukuda, R.; Hasegawa, J.; Ishida, M.; Nakajima, T.; Honda, Y.; Kitao, O.; Nakai, H.; Klene, M.; Li, X.; Knox, J. E.; Hratchian, H. P.; Cross, J. B.; Bakken, V.; Adamo, C.; Jaramillo, J.; Gomperts, R.; Stratmann, R. E.; Yazyev, O.; Austin, A. J.; Cammi, R.; Pomelli, C.; Ochterski, J. W.; Ayala, P. Y.; Morokuma, K.; Voth, G. A.; Salvador, P.; Dannenberg, J. J.; Zakrzewski, V. G.; Dapprich, S.; Daniels, A. D.; Strain, M. C.; Farkas, O.; Malick, D. K.; Rabuck, A. D.; Raghavachari, K.; Foresman, J. B.; Ortiz, J. V.; Cui, Q.; Baboul, A. G.; Clifford, S.; Cioslowski, J.; Stefanov, B. B.; Liu, G.; Liashenko, A.; Piskorz, P.; Komaromi, I.; Martin, R. L.; Fox, D. J.; Keith, T.; Al-Laham, M. A.; Peng, C. Y.; Nanayakkara, A.; Challacombe, M.; Gill, P. M. W.; Johnson, B.; Chen, W.; Wong, M. W.; Gonzalez, C.; Pople, J. A. *Gaussian 03*, Revision C.02; Gaussian, Inc., Wallingford CT, 2004.
- (46) Pohle, W.; Gauger, D. R.; Dornberger, U.; Birch-Hirschfeld, E.; Selle, C.; Rupprecht, A.; Bohl, M. *Biospectroscopy* **2002**, *67*, 499.
- (47) Pilet, J.; Brahms, J. *Biopolymers* **1973**, *12*, 387.
- (48) Scheiner, S. *Hydrogen Bonding*, Oxford University Press: **1997**.
- (49) Hauser, H.; Pascher, I.; Pearson, R. H.; Sundell, S. *Biochimica et Biophysica Acta* **1981**, *650*, 21.
- (50) Gaverzotti, A. *J. Phys. Chem.* **1991**, *95*, 8948.
- (51) Jeffrey, G. A. *J. Mol. Struct.* **1999**, *485–486*, 293.
- (52) Bechinger, B.; Seelig, J. *Chem. Phys. Lipids* **1991**, *58*, 1.
- (53) Ulrich, A. S.; Watts, A. *Biophys. J.* **1994**, *66*, 1441.
- (54) Lewis, R. N. A. H.; Pohle, W.; McElhaney, R. N. *Biophys. J.* **1996**, *70*, 2736.
- (55) Gauger, D. R.; Selle, C.; Fritzsche, H.; Pohle, W. *J. Mol. Struct.* **2001**, *25*, 565.
- (56) Pohle, W.; Bohl, M.; Boehlig, H. *J. Mol. Struct.* **1991**, *242*, 333.